Soft Matter

Dynamic Article Links

Cite this: *Soft Matter*, 2012, **8**, 260

www.rsc.org/softmatter

REVIEW

Shear-thinning hydrogels for biomedical applications

Murat Guvendiren, Hoang D. Lu and Jason A. Burdick*

Received 5th August 2011, Accepted 28th September 2011
DOI: 10.1039/c1sm06513k

Injectable hydrogels are becoming increasingly important in the fields of tissue engineering and drug delivery due to their tunable properties, controllable degradation, high water content, and the ability to deliver them in a minimally invasive manner. Shear-thinning is one promising technique for the application of injectable hydrogels, where preformed hydrogels can be injected by application of shear stress (during injection) and quickly self-heal after removal of shear. Importantly, these gels can be used to deliver biological molecules and cells during the injection process. This review aims to highlight the range of injectable shear-thinning hydrogel systems being developed, with a focus on the various mechanisms of formation and shear-thinning and their use in biomedical applications.

1. Introduction

Hydrogels are three-dimensional polymeric networks that can absorb a large amount of water while maintaining their structural integrity. Hydrogels are perfect candidate soft materials for many biomedical applications including as cell culture substrates and scaffolds for tissue regeneration,[1–7] for cell encapsulation and delivery,[2,4,8–11] for drug and protein delivery,[12–15] as bioadhesives and biosealants,[16–19] and for biomedical devices[20–22] due to their ability to mimic many physical properties of tissues, biocompatibility, potential responsiveness to small environmental changes (*e.g.*, temperature, pH, and ion concentration), and their ability to store functional chemicals and nanoparticles. Among various hydrogel properties, *injectability* is a major requirement for minimally invasive surgery, particularly in tissue engineering and drug delivery applications.

Injectable hydrogels can be easily applied through a syringe and undergo a rapid sol–gel transition at the target site. They can readily take the shape of a cavity, providing a good fit and interface between the hydrogel and tissue. Moreover, various therapeutic molecules and even cells can be incorporated by simply mixing with the precursor solution prior to injection.

Injectable hydrogels can be classified under two main groups according to the nature of their *in situ* cross-linking mechanism,

Department of Bioengineering, University of Pennsylvania, 240 Skirkanich Hall, 210 S. 33rd Street, Philadelphia, PA, 19104, USA. E-mail: burdick2@seas.upenn.edu; Fax: +215-573-2071; Tel: +215-898-8537

Murat Guvendiren

Murat Guvendiren received his BS degree in 2000 and his MS degree in 2003 in Metallurgical and Materials Engineering from the Middle East Technical University, Ankara, Turkey. He obtained his PhD under the supervision of Dr Kenneth R. Shull in the Department of Materials Science and Engineering at the Northwestern University in 2007. Following postdoctoral research with Dr Shu Yang, in 2008, he started working with Dr Jason A. Burdick, in the Department of Bioengineering, University of Pennsylvania, as a postdoctoral researcher. His current research is focused on development of dynamic polymeric material platforms for biomedical applications.

Hoang D. Lu

Hoang D. Lu is currently a Bioengineering graduate student at the University of Pennsylvania under the supervision of Dr Jason Burdick. He earned his B.S. in Chemical Engineering at Columbia University in 2010. His work focuses on protein and molecular engineering of biomedical systems.

namely chemically and physically cross-linked hydrogels. *In situ* chemical cross-linking is commonly obtained *via* photo-initiated, redox-initiated or Michael-type addition polymerization, whereas physically cross-linked hydrogels self-assemble under external stimuli and do not rely on covalent bond formation.[7,23] Temperature,[24–26] pH,[27,28] ion concentration,[29,30] and hydrophobic interactions[31–33] are examples of the most widely studied external stimuli for self-assembly. Some of these physical hydrogels exhibit both viscous flow under shear stress (*shear-thinning*) and time dependent recovery upon relaxation (*self-healing*), providing an alternative strategy for injectable hydrogel application. Key requirements for injectable hydrogels for biomedical applications include:[7,34,35] (*i*) the injectable solution must flow under modest pressure and set rapidly at the target site; (*ii*) the mechanical properties of the hydrogel must quickly build up after injection; (*iii*) the hydrogel should maintain sufficient integrity and strength as long as necessary; (*iv*) the hydrogel and precursors need to be biocompatible with minimal cytotoxicity; (*v*) the hydrogel should have controlled biodegradability; and finally, (*vi*) the polymer structure should be suitable for molecular design to tune biological functionality of the hydrogel. In this respect, shear-thinning hydrogels provide several advantages over other injectable systems.

Shear-thinning behaviour enables a pre-formed hydrogel with desired physical properties, as characterized *ex vivo*, to be delivered *in vivo via* application of shear stress during injection (most commonly by passing through a syringe). As the hydrogel is pre-formed *ex vivo*, the effect of the local environment on cross-linking is almost negligible, whereas other injectable hydrogels are liquid prior to injection and may be affected by the *in vivo* environment during cross-linking.[36] Additionally, the recovery of elastic modulus after shear (self-healing) may be much faster in shear-thinning hydrogels than the gelation process of other types of hydrogels.[37,38] Finally, purely liquid precursor solutions (*e.g.*, uncross-linked polymers, unreacted radicals) may leak into the neighbouring tissue or dilute with the body fluid,[39,40] which may not only limit the hydrogel formation but also raise toxicity concerns.

Here, we review shear-thinning hydrogels in the context of biomedical applications. First, we highlight the mechanisms for hydrogel formation to obtain shear-thinning behaviour. Following this, shear-thinning systems are reviewed in detail under several sub-groups including peptide-based hydrogels, protein-based hydrogels, hydrogels from blends, colloidal systems, and cyclodextrin-based hydrogels. Hydrogel formation mechanisms, shear-thinning and self-healing properties, as well as applications in the biomedical field are summarized for each sub-group. Although the application of shear-thinning injectable hydrogels in biomedicine is fairly new and currently limited to primarily *in vitro* studies, the majority of shear-thinning hydrogels are particularly suitable for cell and drug encapsulation and delivery.

2. Criteria for shear-thinning hydrogels

Self-assembly is the main route for cross-linking for shear-thinning hydrogels. The mechanism of the self-assembly process is specific to the shear-thinning system and thus given in detail under each shear-thinning hydrogel sub-section below. Briefly, self-assembly in many of these systems is obtained as a result of a balance between competing forces that favor assembly (*e.g.*, hydrophobic interactions, hydrogen bonding and electrostatic attraction) and forces that act against assembly (*e.g.*, electrostatic repulsion and solvation).[41] These interactions are generally weak individually but collectively they can lead to formation of stable network structures. Due to the dynamic nature of these weak physical associations, formed networks can be dissociated under applied shear. Shear-thinning process is highly nonlinear, and can be indicated by a non-sinusoidal response under sinusoidal applied shear. When shear is removed, these networks then reassemble into hydrogels. The hydrogel modulus and shear-thinning/self-healing kinetics are important parameters that determine the suitability of the system for biomedical applications. For instance, during drug delivery slow recovery rates may lead to sedimentation or leakage of the encapsulated cargo. For cellular delivery, in addition to recovery rate the amount of applied shear is also crucial for cell survival. The shear rate near the needle wall can be much higher than that at the centre, therefore it is possible for the material near the wall to undergo shear-thinning while the material at the centre retains an intact network structure. Although this allows cellular delivery, cell viability observed at the centre may not necessarily prove that cells can survive the shear stress.

3. Classes of shear-thinning hydrogels

Hydrogels with shear-thinning ability comprise a relatively large group of polymeric systems, and their shear-thinning and physical properties have been well reviewed.[42–50] Here, we focus on shear-thinning hydrogels utilized for biomedical applications under five main groups: (*i*) peptide-based hydrogels, (*ii*) protein-based hydrogels, (*iii*) hydrogels from blends, (*iv*) colloidal systems, and (*v*) hydrogels based on cyclodextrins and block copolymers. For each system, we provide a detailed review of the material design, shear-thinning and self-healing properties, and investigated biomedical applications.

Jason A. Burdick

Jason A. Burdick is an Associate Professor in the Department of Bioengineering at the University of Pennsylvania. The focus of work in his laboratory is the development of biodegradable polymers for tissue engineering and drug delivery. He has received a K22 Award from the National Institutes of Health, a Fellowship from the Packard Foundation, an Early Career Award from the Coulter Foundation, and a CAREER Award from the National Science Foundation. He has published over 95 papers and is on the editorial boards of the Journal of Biomedical Materials Research A, Biomacromolecules, ACS Applied Materials and Interfaces, Biomedical Materials, *and* Tissue Engineering.

3.1. Peptide-based hydrogels

Self-assembling peptides are well suited for forming shear-thinning networks as the unique physical properties and diversity of the natural occurring amino acids allow incorporation of various non-covalent interactions such as electrostatic, hydrophobic, π-stacking, hydrogen bonding and conformal changes.[51] Moreover, the ease of sequence specific modifications of the peptides at the molecular level is a significant advantage, which enables researchers to fine tune the physical properties of the hydrogel, such as crosslinking density, mesh size, hydrophobicity/hydrophilicity, net charge (electrostatics) and degradation rate.[52]

Over the last ten years, Pochan and Schneider and coworkers have developed a family of self-assembling β-hairpin peptides, namely 'MAX' peptides, and investigated their properties as injectable therapeutic delivery vehicles.[37,53–57] These peptides contain two blocks of alternating hydrophobic and basic amino acids linked together by a Val^{D}-Pro-Pro-Tyr type II′ β-turn forming spacer. The widely studied MAX1 peptide contained a $(Val\text{-}Lys)_4$-Val^{D}-Pro-Pro-Tyr-$(Val\text{-}Lys)_4$ sequence. These peptides were disordered when Lys residues were protonated, and electrostatic repulsion of peptide amino acid sequences prevented any inter- or intra-molecular association.[57,58] When charge repulsion between Lys amino acids were reduced by increasing the acidity of the solution or increasing ionic shielding, peptide strands were shown to fold into β-hairpins due to intramolecular bonding, displaying a hydrophobic and a hydrophilic face in β-hairpin configuration (Fig. 1a). Hydrophobic association of two hairpins formed units that were 20 Å high and 32 Å wide. These units laterally grew with other hairpin pairs *via* hydrogen bonding as well as hydrophobic association.[55] This led to the formation of long fibrils (up to 200 nm), inducing a sol–gel transition (Fig. 1a). Gelation at constant temperature was induced by neutralizing the peptide charge by titrating the pH from basic to neutral.[59] Gelation at physiological pH was obtained by shielding the electrostatic repulsion between peptides by either gradually increasing the salt concentration (∼150 mM NaCl) to shield peptide charges[60] or by increasing the temperature to strengthen the hydrophobic interactions.[54]

The ability to self-assemble under physiological conditions makes these peptide-based hydrogels attractive for cellular encapsulation and delivery. When cells in growth media were mixed with MAX peptide dissolved in deionized water, the salts in the growth media triggered fibril formation and gelation to encapsulate the cells under mild conditions. For instance, MAX1 gels (2 wt%) constituted in Dulbecco's Modified Eagle's Medium formed robust hydrogels (shear modulus ∼1kPa) that recovered back to their initial modulus within 5 min post-shearing.[37] A detailed investigation of the shear-thinning behaviour of these gels *via* rheo-small-angle neutron scattering and small angle X-ray scattering showed formation of nano gels (200 nm) due to shear banding and fracture during shear-thinning (Fig. 1b).[36]

MAX peptides were shown to be cytocompatible with NIH 3T3 murine fibroblasts, C3H10t1/2 mesenchymal stem cells (MSCs), primary articular chondrocytes, hepatocytes, and MG63 osteoblast progenitor cells.[36,37,61–63] For example, fibroblasts cultured in MAX1 gels (2 wt%) were viable but proliferated ∼25 to 50% slower than fibroblasts cultured on tissue culture treated polystyrene (TCPS), yet they still exhibited a spread morphology within fifteen minutes and became confluent within three weeks.[64] MSCs and osteoblast progenitor cells encapsulated in MAX gels remained mostly viable after shearing through a needle (18 $^{1}/_{2}$ or 20 gauge needle) into growth media.[36,37] Moreover, a homogenous distribution of the encapsulated cells was observed after injection, illustrating the sustainability of cellular distribution during shear-thinning and

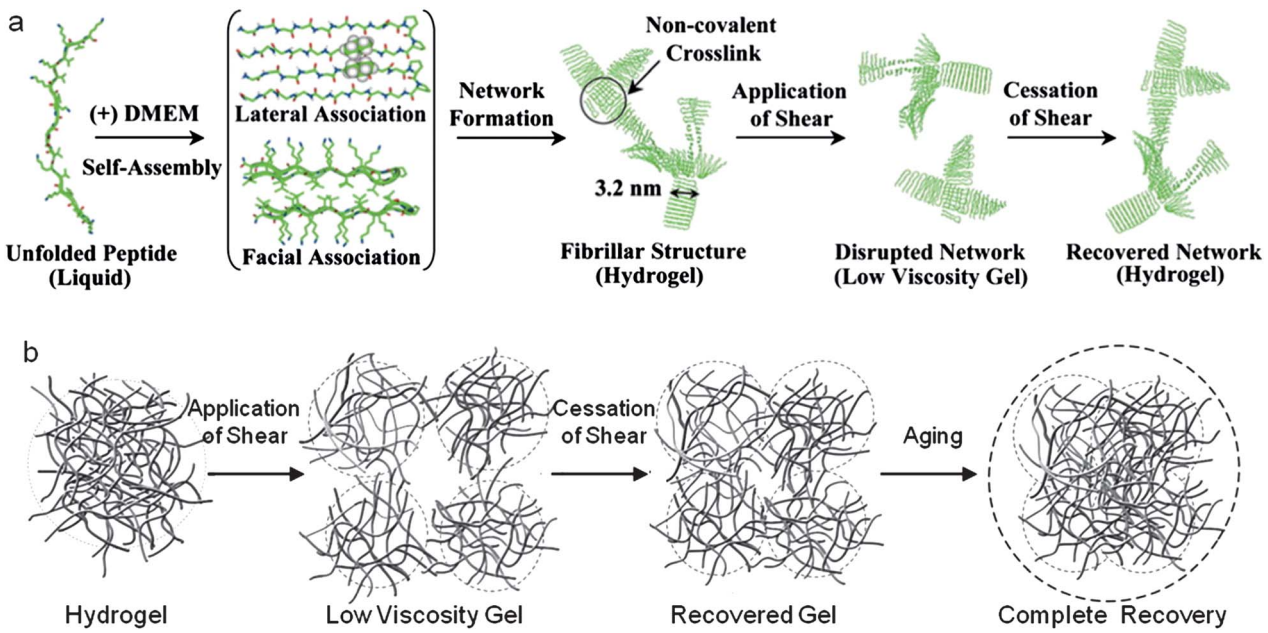

Fig. 1 (a) Self-assembly, shear-thinning and self-healing mechanism of β-hairpin peptide-based fibrillar hydrogel. Reproduced from Haines-Butterick *et al.*, ref. 37, with permission. (b) Schematic of network structure evolution during shear-thinning and recovery from shear. Reproduced from Yan *et al.*, ref. 36, with permission.

following the self-healing process. To investigate the pro-inflammatory response of the MAX gels, macrophages (J774 mice peritoneal macrophages) were cultivated on MAX gels.[64] The measured secreted pro-inflammatory cytokine tumor necrosis factor-α were at levels similar to those of macrophages on TCPS, without observed differences in the macrophage viability and morphology. Although MAX gels were cytocompatible and biocompatible with mammalian cells, they were shown to be toxic to bacteria (*e.g.*, gram-positive *Staphylococcus epidermidis*, *Staphylococcus aureus*, and *Streptococcus pyogenes*, and gram-negative *Klebsiella pneumoniae* and *Escherichia coli*), which is believed to be a result of bacterial membrane disruption by MAX1.[65] This behaviour might help reduce the risk of infection after surgical delivery of the MAX1 gels. MAX gels were also reported to enhance drug payloads for delivery in a localized and controlled fashion.[66] For instance, the anti-inflammatory drug corcumin was shown to prevent tumor growth and spreading, but its maximum single drug dose and effects are limited because of poor solubility in aqueous solutions.[67–70] MAX gels were reported to solvate corcumin by 'caging' the drug from interactions with hydrophobic peptide residues. The growth of cancerous human medulloblastoma cells was inhibited when cells were cultured on corcumin containing MAX gels, but was not affected when cultured on MAX gels alone.[66] Drug dosing amount, drug release profiles, and inhibition of cancerous cell growth were shown to be tuned by varying the peptide weight percent of MAX gels.

The MAX peptide system is highly versatile and the properties of self-assembled hydrogels can be easily tuned *via* molecular engineering. When a bulky and photocleavable α-carboxy-2-nitrobenzyl (CNB) functional group was incorporated into the peptide sequence, hydrogen bonding that is required for β-hairpin stabilization was prevented due to CNB steric hindrance.[53] Sol–gel transitions at physiological pH and temperature could be controlled and triggered by photocleaving CNB from MAX7CNB, which led to peptide folding and fibril formation *via* UV exposure. Gelation kinetics and gel strength could also be tuned by changing the primary amino acid sequence. MAX peptides containing unnatural sorbamide modified amino acids self-assembled into gels with physical properties similar to other MAX gels, but may be further stiffened by covalently cross-linking the network *via* photopolymerization of dienes on the sorbamide groups.[71] This modification allowed the MAX gel elasticity and stability to be tuned after shear-induced injection. When a single Lys amino acid was substituted with a Glu amino acid on MAX1, the time required for this new MAX8 peptide to complete β-sheet formation (self-assemble) was significantly reduced from ~30 min to less than a minute.[37] This substitution with a single negatively charged amino acid on the MAX peptide facilitated β-hairpin and fibril formation by reducing electrostatic repulsion between positively charged Lys groups. For instance, the storage modulus of MAX8 (0.5 wt%) reached 100 Pa within a minute after being induced with a gelation stimulus, whereas MAX1 (0.5 wt%) did not reach 40 Pa even an hour after being similarly induced.[37] This decreased gelation time allowed cells to be homogenously encapsulated and reduced issues with cell sedimentation and cell loss when compared with MAX1 gels (Fig. 2a–b). Cells within MAX8 gels were shown to retain their homogeneous distribution after injection (Fig. 2b–c). Additionally, substitution of the two Lys residues on MAX1 with Arg on MARG1 was reported to enhance the gel antimicrobial properties.[72] For instance, MARG1 peptides can inhibit methicillin resistant *Staphylococcus aureus* growth at loading densities of over 10^8 colony forming units dm^{-2}, while MAX1 can inhibit growth at loading densities up to only 10^5 colony forming units dm^{-2}. It is suggested that Arg on MARG1 disrupts bacterial membranes more proficiently than Lys on MAX1. Recently, MAX1 has been engineered to have an additional β-turn and sheet forming domain.[73] These new three-stranded β-sheet forming peptides (TSS1) are cytocompatible with MSCs and formed stronger hydrogels, with 2 wt% gels having a plateau modulus of up to 8.5 kPa.

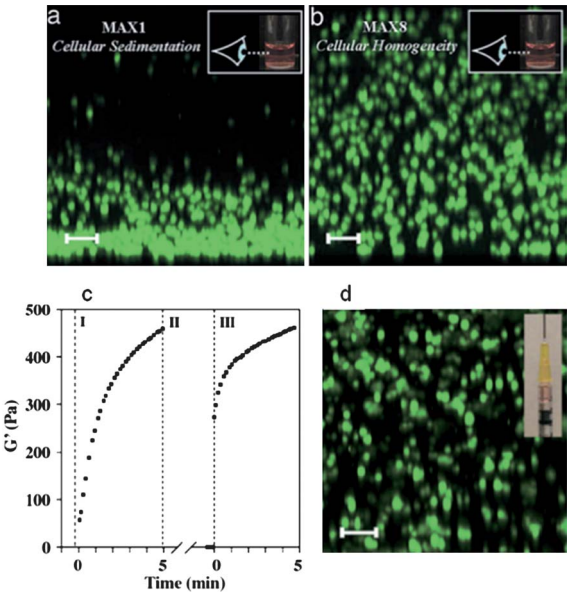

Fig. 2 (a–b) Confocal z-stack images of MSCs encapsulated in MAX1 and MAX8 hydrogels. (c–d) Self-healing kinetics and MSC distribution in MAX8 gels after injection. Inset shows the image of hydrogel in the syringe prior to injection. Cells were labeled with cell tracker (green). Scale bars are 100 microns. Reproduced from Haines-Butterick *et al.*, ref. 37, with permission.

Recently, self-assembling 'multidomain peptides' (MDPs) were used to construct shear-thinning and self-healing hydrogels.[74] These peptides have an ABA block motif, where the B block is a series of (Gln/Ser)-Leu repeats, and the terminal A blocks are positively charged Lys or negatively charged Glu. The hydrophilic Gln/Ser residues organize onto one face of the B block, and the Leu residues position themselves onto the opposite face. The hydrophobic faces on this amphiphilic B block pack together into β-sheet and fibril forming peptide sandwiches (Fig. 3).[75–78] When fused to flanking A blocks, the electrostatic repulsion between positively or negatively charged A blocks limits sheet formation. When charge repulsion between A blocks on MDPs were reduced, MDPs folded into β-sheet forming fibers (2 nm high, 6 nm diameter wide, and 120 nm long). Gelation of MDPs could be induced by either protonating or deprotonating the charged A blocks by pH titration or *via* charge shielding from increasing salt concentration. When the A blocks consisted of

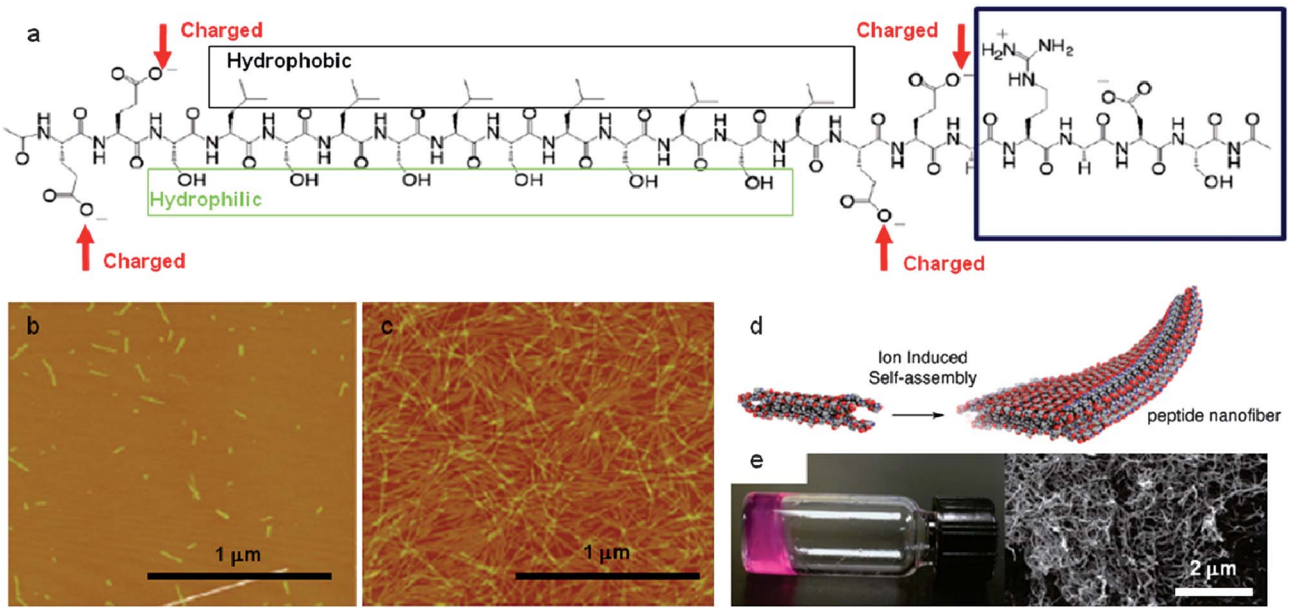

Fig. 3 MDPs self-assemble into nanofibrous hydrogels. (a) Chemical structure of MDP nanofiber used in this study. (b) Short nanofibers after first step of self-assembly as visualized by AFM. (c) Cross-linked nanofibers after gelation with Mg^{2+}. (d) Illustration of the assembled nanofibers. (e) Fibrous hydrogel of the MDP as formed in the cell culture media (right), and corresponding SEM image. Reproduced from Bakota *et al.*, ref. 81, with permission.

negatively charged poly-Glu, the gelation was induced by the addition of divalent cations such as Mg^{2+}.[41] $Glu_2(Ser\text{-}Leu)_6Glu_2$ MDP gels (1%) in the presence of Mg^{2+} were reported to have a storage modulus near 480 Pa, and recovered 75% of their original modulus within 13 s after shear-thinning.[41,74] Gels were fully recovered (reaching its original modulus) within 10 min.

MDPs provided an alternate platform for cytocompatible cell and drug delivery.[79] For instance, MSCs from human exfoliated deciduous teeth (SHED)[80] cultured in MDP gels exhibited a steady increase in their rate of metabolic activity, as determined by MTT assays, for at least two weeks, indicative of proliferation. Moreover, when the A domain was modified with Arg-Gly-Asp, a cell adhesion site, SHED metabolic activity within MDP gels was increased up to three times that of SHED in unmodified MDP gels. Furthermore, magnetic resonance imaging of gadolinium labelled MDP gels injected into the cavity of mice showed that gels remained intact and at the site of delivery for at least 24 h.[81] These observations showed that the MDP gels provided robust and rapid self-healing properties to deliver the cells at localized and targeted areas. MDPs were also used as 'sponges' to absorb drugs for subsequent delivery. For instance, MDP gels were shown to absorb the stem cell secretome when human H9 embryonic stem cells were cultured across MDP gels, separated by a protein permeable membrane.[82–84] Renal microvascular endothelial cells cultured in the presence of such conditioned MDP gels exhibited lower levels of apoptosis and hyperpermeability when subjected to a deleterious lipopolysaccharide treatment in an endotoxemia model.[76] Similar treatment with non-conditioned MDP gels did not show any therapeutic benefits. Furthermore, acute kidney damage in male $Rock1^{-/-}$ mice from lipopolysaccharide treatment was also reduced when the mice were treated with an intraperitoneal injection of conditioned MDP gels.[85]

Cell secretome delivery by MDP 'sponge' vehicles has several advantages. Cell free systems have lower risk of immunological rejection and cancerous teratoma formation, when compared to therapies involving embryonic stem cell delivery.[86] This strategy can be broadly applied to other organ systems, such as for cardiac repair.[87] The modular design of MDP blocks allows MDP gels to be highly tunable through variations in block amino acid sequence or length. For example, the incorporation of disulfide bridge forming cysteines in the B block can greatly increase the storage modulus, with 1 wt% $Glu_2(Cys\text{-}Leu\text{-}Ser\text{-}Leu)_3Glu_2$ gels having storage moduli up to around 6100 Pa. MDPs with B blocks designed to contain a matrix metalloproteinase 2 cleavable site formed gels that could be enzymatically degraded and that were more supportive of cellular proliferation.[79]

In another example, a system utilizing a pair of self-repulsive but mutually attractive peptides was developed to construct shear-thinning and self-healing hydrogels.[88] One peptide had a repeating polar positive-hydrophobic neutral amino acid motif (acetyl-Trp-Lys-$(Val\text{-}Lys)_4$-amide) and the second peptide had a repeating polar negative/hydrophobic neutral amino acid motif (acetyl-Glu-Trp-$(Glu\text{-}Val)_4$-amide). Acetyl and amide modifications were made to eliminate natural *N*- and *C*- termini charges and reduce self-attraction. In isolation, these peptides exhibited random coil structure. When mixed together, peptides co-assembled into micrometre long fibrilar structures and underwent a sol–gel transition. Hydrogels (0.25 wt%, pH 6.0) had a storage modulus $\sim 10^3$ Pa, and required approximately half an hour to recover to 90% of their initial modulus after being sheared. Gels maintained physical fidelity even after 30 cycles of shearing and recovery. Gel properties could be tuned by changing peptide length, sequence, and weight percent.[88]

These gels were used to encapsulate proteins by simply mixing peptide components with the cargo.[89] For instance, lysozyme and ubiquitin retained native tertiary structures and surface chemistry when encapsulated in this manner, but displayed altered surface chemistry when encapsulated by pH triggered gelation. These mix-gelation systems may be advantageous to encapsulate cargo under constant conditions by limiting unintentional gelation due to ionic fluctions that some uni-peptide systems suffered from.[90] However, these hydrogels are not yet suitable for cellular studies as the pH of hydrogels (pH 6.0) was below physiological conditions.

3.2. Recombinant protein-based hydrogels

Protein-protein interaction between specific peptide domains is a well recognized concept to develop molecular recognition based physical hydrogels. Likewise, recombinant proteins are promising and highly versatile building blocks to develop shear-thinning hydrogels for biomedical applications. While peptides synthesized with traditional solid-phase chemistry methods are limited to tens of amino acids in size, proteins produced with cell expression systems can be significantly larger and may exhibit more advanced biological activity.[49,91] Additionally, recent advances in molecular biology and oligonucleotide synthesis significantly improved the ability to develop recombinant protein systems.[92] It is now possible to commercially synthesize customized and cell-expression ready DNA constructs at affordable rates. Moreover, recombinant proteins from genetically engineered protein encoding DNA sequences could possess synergistic combinations of self-assembly, stimulus-response, catalytic, structural, and chemical functionalities.[51]

Recombinant proteins based on WW domain and proline-rich peptide motifs were engineered to develop two-component molecular recognition physical hydrogels that self-assemble at constant physiological conditions and show shear-thinning properties (Fig. 4).[93] WW domains are small (30–50 amino acid long) triple stranded antiparallel β-sheet structures with two highly conserved tryptophans.[94–96] Intracellular WW domains containing proteins regulate metabolic and gene function by binding to Pro-Pro-X-Tyr motifs with micromolar binding affinities (K_d).[97,98] Binding is conferred primarily from hydrophobic interactions between peptide residues on the WW domain groove orthogonal to its β-sheet strands, and binding specificity across various WW domains are based largely on structural and charge variations within the groove binding sites. Poly-WW-domain molecules and poly-Pro-Pro-X-Tyr molecules can undergo a sol–gel transition when combined together *via* a so-called mixing-induced, two-component hydrogel (MITCH) gelation mechanism.[93] The two components bind to each other when mixed, and form random intermolecular cross-links, resulting in a sol–gel transition (Fig. 4). A large library of proline-rich peptide association domains was available with varying degrees of binding specificity and strength. Therefore, the bulk rheological properties of the hydrogels, such as kinetics of self-healing, could be easily tailored *via* molecular design. For instance, Foo *et al.* reported that for MITCH hydrogels after shear-thinning with the stronger binding peptide (C7:P9), complete self-healing was achieved within 5 min, whereas the weaker binding peptide (N7:P9) required 30 min to self-heal (Fig. 5).[93]

Gels formed from the MITCH mechanism were cytocompatible with human umbilical vein endothelial cells, murine adult neural stem cells, and PC-12 neuronal-like cells.[93] Although previous studies showed that relatively weak 2D hydrogels (shear modulus, $G' \sim 10$Pa) did not support adult neural stem cell (NSC) self-renewal and differentiation,[99] 3D MITCH gels ($G' \sim 9$–50 Pa) were shown to support encapsulated NSC differentiation and proliferation (Fig. 5).[93] The MITCH gels are advantageous as cells and other therapeutic cargo can be encapsulated under mild conditions with constant pH, salt concentration, and temperature, preserving the therapeutic effects of sensitive cargo. Additionally, the cross-linking domains are highly specific for each other, which limits the probability of non-specific interactions with cellular and matrix components. However, some of the disadvantages of systems requiring protein expression are relatively low protein yields (typically <50 mg L^{-1} culture), extensive purification steps, and risk of endotoxin contamination.

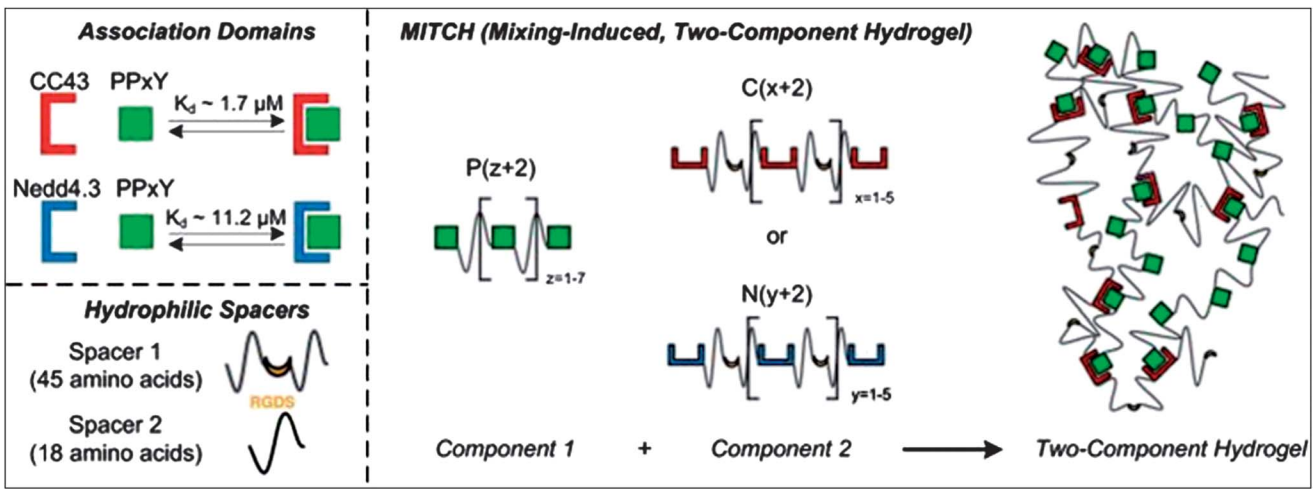

Fig. 4 Schematic of mixing-induced, two component hydrogel self-assembled *via* molecular recognition mechanism. WW domains (CC43 and Nedd4.3) bind the proline peptide (PPxY) (Top left). Multiple repeats of WW domains were linked by hydrophilic spacers (Bottom left). Hydrogel was formed by mixing component 1 with component 2 (either C[x + 2] or N[y + 2]). Reproduced from Foo *et al.*, ref. 93, with permission.

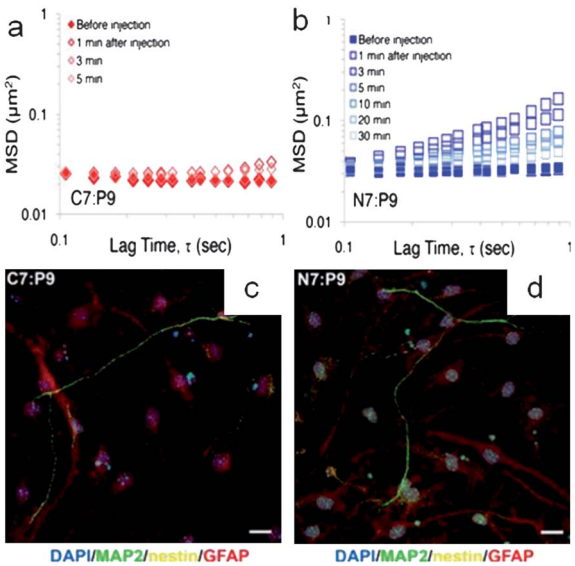

Fig. 5 (a–b) Self-healing kinetics after shear-thinning for hydrogels with stronger-binding (C7:P9) and weaker-binding (N7:P9) domains. (c–d) Confocal z-stack projections of neural stem cells differentiated within two-component hydrogels (C7:P9 and N7:P9 gels (5 wt%)) at day 6 (red, glial marker GFAP; green, neuronal marker MAP2; yellow, progenitor marker nestin; blue, nuclei, DAPI). Scale bars are 25 microns. Reproduced from Foo *et al.*, ref. 93, with permission.

Recombinant proteins based on leucine-zipper based domains were also used to develop shear-thinning hydrogels. Leucine-zippers contain an (abcdefg) motif, in which the residues in 'a' and 'd' positions are hydrophobic (and generally Leu), and the residues in 'e' and 'g' positions are charged (Fig. 6).[100] This motif supports formation of amphiphilic α-helices, and parallel strands can bind each other to induce aggregation between their hydrophobic faces. This motif is used to link proteins, DNA, and transcription factors within the cell. Shear-thinning hydrogels were reported from a recombinant tri-block protein consisting of two leucine-zippers linked together by a soluble polyelectrolyte peptide domain.[101] The leucine-zippers were shown to form trimeric and tetrameric aggregate bundles that act as physical cross-linking domains, and formed a network structure at high concentrations under physiological conditions (Fig. 6).[102–104] Furthermore, α-helix secondary structure and bundle formation were disrupted at exceedingly high or low pH, and gelation was generally induced from an acidic to physiological pH shift. These hydrogels also exhibited very fast self-healing kinetics. For instance, after being shear-thinned at physiological conditions, 7 wt% gels (with a modulus ~1 kPa) recovered their original modulus in less than a minute.[40]

These hydrogels were shown to be cytocompatible with human fibroblasts, where cells exhibited polarized morphology with mature actin stress fibers when the hydrophilic linker was modified with Arg-Gly-Asp, an integrin binding sequence, and remained rounded on unmodified hydrogels.[104] These triblock proteins were shown to easily absorb to glass, polystyrene, and polyesters to develop bioactive surface coatings, which can modulate cellular behaviour.[105] Moreover, the viability and proliferation of human fibroblasts, human umbilical vein endothelial cells, and rat neural stem cells increased when cultured on protein treated surfaces by providing integrin binding sites, compared to cells cultured on unmodified surfaces.

Similar to other peptide- and protein-based hydrogels, recovery times, physical properties, and bioactivity of hydrogels from leucine-zipper based domains can be easily tuned. For instance, pH, salt concentration and temperature directly affect protein surface charge, shielding of charges, strength of protein associations, propensity of bundle dissociation, expansion and swelling of the midblock linker, and tendency of loop formation.[106] These can then be used to adjust plateau moduli, relaxation times, and erosion rates.[106] Moreover, the sequence of the leucine-zipper and linker can be changed to tune gel properties. For example, extending the length of the polyelectrolyte spacer, using dissimilar endblock leucine-zippers, or adding a disulfide bridge forming cysteine to one leucine-zipper block was shown to repress loop formation, decreasing the rate of erosion by three orders of magnitude.[107,108] This allowed the release of large encapsulated therapeutic agents at a linear rate, which was correlated with the erosion rate, from within hours to months.[107,108] It is also possible to bio-functionalize the hydrogels by incorporating proteins between leucine-zipper blocks. GFP,

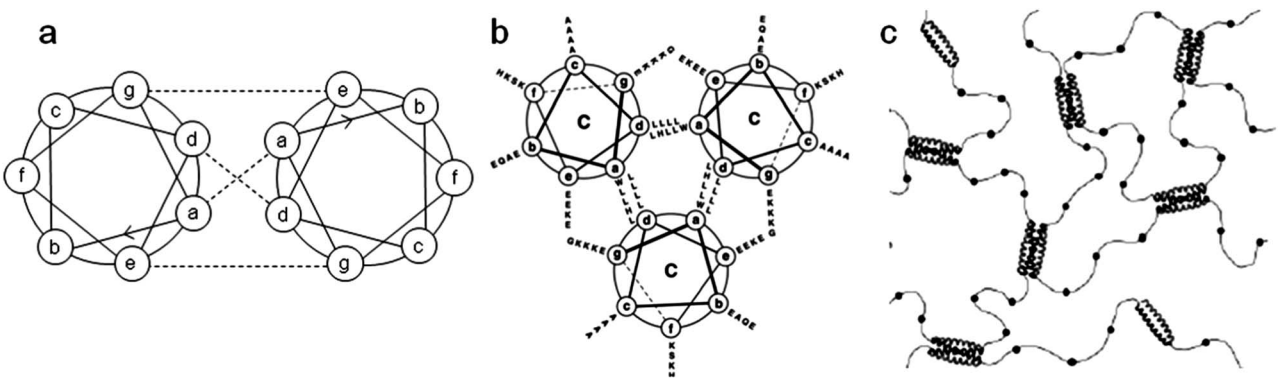

Fig. 6 (a) Helical wheel containing an (abcdefg) motif. Residues in 'a' and 'd' positions are hydrophobic, and the residues in 'e' and 'g' positions are usually charged. (b) Helical wheel representation of a trimeric leucine zipper bundle. Reproduced from Fischer *et al.*, ref. 105, with permission. (c) Schematic of leucine zippers connected by integrin binding ligand (filled circles) containing peptide linkers cross-linking into a hydrogel from bundle formation. Reproduced from Mi *et al.*, ref. 104, with permission.

dsRED, and ECFP, fused between leucine-zippers led to the formation of hydrogels with fluorescent activity, whereas modification with organophosphate hydrolase and aldo-keo reductase led to gels with catalytic activity.[109–111] Moreover, a system utilizing leucine-zippers fused to calmodium allows a sol–gel transition to be induced by the addition of calcium ions.[112] This system is particularly important as it may allow cells to be encapsulated under relatively mild conditions without the need for pH shifts. Additionally, leucine-zippers functionalized with a spacer and terminal acrylate group can undergo sol–gel transition with UV light exposure *via* photopolymerization.[113]

3.3. Hydrogels from blends

Different polymeric materials with thermal-responsive, shear-thinning, shape memory, and biological properties can be combined to yield composite hydrogels with improved properties for biomedical applications. For instance, hyaluronic acid (HA) was blended with methylcellulose (MC) to form injectable HAMC hydrogels that flow under shear.[114] MC is a liquid at room temperature with inverse thermal gelling properties, and undergoes a sol–gel transition post *in situ* injection from warming up to body temperature.[115] The gelation of MC (9 wt%) takes ~10 min after injection, which may lead to dispersion of cargo and a decrease in delivery yield when used as a delivery vehicle.[114] However, blending HA (2 wt %) with MC (7 wt%) significantly reduced the gelation time to less than 2 min. HAMC blends formed hydrogels at room temperature due to dehydration of MC by anionic carboxylic acid groups on the HA. HAMC hydrogels also had shear-thinning properties due to the entangled random coil structure of HA. HAMC hydrogels were shown to have a higher modulus post-injection due to the inverse thermal gelation properties of MC.[114]

3T3 fibroblasts cultured on HAMC gels showed minimal gel adhesion or cell spreading, and primarily adhered to each other to form cell clusters. Rats subjected to laminectomy[116] and injured by spinal cord compression[117] showed improved locomotive function when HAMC was injected at the site of injury, when compared with injections of artificial cerebrospinal fluid. HAMC hydrogels were also used as a shear-thinning injectable drug carrier. For instance, the solubility of a hydrophobic neuroprotectant drug nimodipine was over an order of magnitude higher in HAMC gels than in simple aqueous solutions, increasing the soluble drug load concentration.[118] The release rates of nimodipine solubilized in HAMC gels were higher than suspended crystalline nimodipine. Suspensions of fast released solubilized nimodipine and slow released crystalline nimodipine in HAMC gels led to a biphasic drug release profile. The solubility and rapid-phase release of nimodipine could be further tuned by varying HAMC gel composition.

Chitosan, silicate laponite-RD (LRD) nanodisks, and poly (ethylene oxide) (PEO) blends have also been used to form injectable shear-thinning and self-healing hydrogels for tissue engineering purposes. For this purpose, PEO was physically absorbed onto the silicate nanodisk surfaces and formed a physically cross-linked structure.[119–121] Although the exact nature of PEO-LRD interactions are not completely understood, it is believed that ionic and hydrogen bonding between mixed components plays a great role in these interactions.[122] Chitosan, previously shown to promote cell adhesion, growth, and wound healing, was added to the gel to enhance their biological properties.[123–125]

3T3 fibroblasts were shown to be cytocompatible with PEO-LRD gels. Fibroblasts exhibited rounded morphologies on gels with low LRD content, but displayed an increasingly spread morphology with increasing LRD concentration.[126] Fibroblast proliferation and spreading also increased with increased chitosan content.[127] Albumin protein encapsulated in these gels displayed burst kinetics, and the protein release rates were tuned by varying the LRD and chitosan content.[128] The addition of chitosan to gels also enhanced encapsulated MC3T3-E1 subclone 4 mouse preosteoblast cell proliferation rates, and encouraged differentiation into osteoblasts.[129]

3.4. Colloidal systems

Shear-responsive colloidal gels composed of two-component self-assembling poly(D,L-lactic-*co*-glycolic acid) (PLGA) based nanoparticles were recently used as tissue engineering scaffolds and drug delivery vehicles.[130–132] In this system, the two oppositely charged nanoparticles of PLGA, namely PLGA coated with positively charged polyvinylamine (PLGA-PVAm, ~180 nm) and with negatively charged poly(ethylene-*co*-maleic acid) (PLGA-PEMA, ~145 nm), self-assembled due to favourable electrostatic attraction (Fig. 7a).[133–135] The assembly was an interconnected ring-like structure yielding a porous and organized network (Fig. 7b). The network was shown to be destroyed under shear stress, and spontaneously self-healed upon removal of shear, allowing these gels to be molded into different geometries (Fig. 7c). The mechanical properties of the gels were determined by the relative compositions of PLGA-PVam and PLGA-PEMA. These gels also maintained their network structure when submerged in excess growth media for two weeks.[130,132]

Human umbilical cord matrix stem cells (hUCMSCs) cultured on these substrates were highly viable and exhibited a well-spread morphology, demonstrating their cytocompatibility and conductivity to cellular adhesion.[132] Furthermore, near-zero dexamethasone release was reported over 2 months when the drug was loaded in the PLGA nanoparticles and simply blending the drug with the particles showed similar kinetics for 1 month.[131] Moreover, injection of PLGA-PVAm/PLGA-PEMA gels (with or without dexamethasone) into cranial defects supported osteoconductive bone formation, whereas the untreated cranial defects showed negligible bone formation and collapsed.[131]

A similar system utilizing oppositely charged gelatin nanospheres was developed.[136,137] These systems form physically robust colloidal gels, are relatively inexpensive, and rely on non-specific electrostatic interactions. Moreover, the mechanical properties of these gels are readily tuned by varying pH and charge shielding by tuning salt concentration. However, due to the non-specific nature of the cross-linking interactions, these gels may also interact with charged molecules and ECM components found in the native tissue.

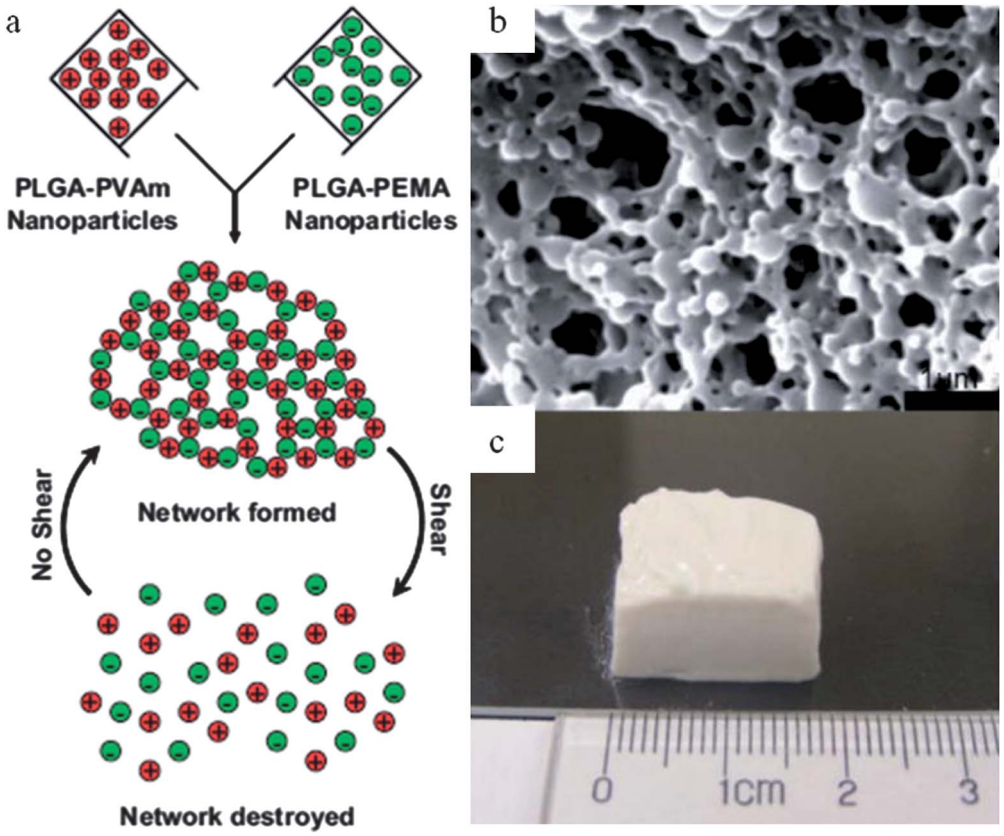

Fig. 7 (a) Schematic showing the self-assembly, shear-thinning and self-healing mechanism of colloidal gels. Reproduced from Wang *et al.*, ref. 130, with permission. (b–c) SEM image (b) and a picture of a colloid gel (c). Scale bar is 1 micron. Reproduced from Wang *et al.*, ref. 131, with permission.

3.5. Hydrogels based on cyclodextrins (CDs) and block copolymers

Another group of shear-thinning hydrogels is based on the self-assembly of the inclusion complexes between cyclodextrin (CD) with biodegradable block copolymers. CDs are natural water-soluble cyclic oligosaccharides of D-glucose units linked by α-1,4-linkages, and named according to the number of anhydroglucose units involved, such as α-, β-, or γ-CD for 6, 7, or 8 D-glucose, respectively (Fig. 8a).[138,139] The 3-dimensional structure of these CDs resemble a truncated cone such that the hydroxyl groups are located at the outer surface, the primary hydroxyls forming the narrow side and the secondary hydroxyls forming the wider side, creating a hydrophobic inner cavity. The inner diameter of the hydrophobic cavity is 0.45, 0.70, 0.85 nm having a depth of 0.67, 0.70 and 0.70 nm for α-, β-, or γ-CD, respectively.[138,139]

Linear polymers such as poly(ethylene oxide) (PEO) can easily penetrate the inner cavity of the CDs to from inclusion complexes (Fig. 8b–c).[140] The inclusion complex formation between CDs and polymers is mainly controlled by the dimensions of the CDs and the cross-sectional areas of the polymer chains, as well as the hydrogen bonding of the neighbouring CDs.[140] For instance, poly(propylene oxide) (PPO) is too large to penetrate the inner cavity of α-CD, but easily penetrates that of β- and γ-CD.[140–142] Moreover, linear water-soluble polymers such as poly(ethylene glycol) and PEO formed inclusion complexes with the smallest size α-CD in high yield, but not with larger β-CD.[143,144] Inclusion complexes are formed when CDs thread onto the polymer chain, and are stabilized by the CD/polymer hydrophobic interactions and hydrogen bonding between CDs. The spontaneous aggregation of these complex structures drives gelation *via* physical crosslinking (Fig. 8c). For strongly hydrophobic polymers, such as poly(ethylene), slow CD threading kinetics hinders complex formation. Therefore, block copolymers composed of hydrophobic and hydrophilic blocks were used to obtain complex stability with moderate threading kinetics. For instance, when poly(ethylene oxide)-poly(propylene oxide)-poly(ethylene oxide) (PEO-PPO-PEO) is used, α-CD is found to slide onto bulky PPO blocks and selectively form inclusion complexes with the middle PEO block.[145] In some cases, hydrogel formation is also supported by the hydrophobic aggregation of the unthreaded polymer blocks, forming more stable structures. For example, in the case of poly(ethylene oxide)-poly[(*R*)-3-hydroxybutyrate]-poly(ethylene oxide) (PEO-PHB-PEO) triblock copolymer, gelation was reported to be inclusion complexation between α-CD and PEO blocks, and aggregation of the hydrophobic PHB block (Fig. 8d–e).[146] A series of PEG grafted polysaccharides including dextran,[147] chitosan[148] and hyaluronic acid[149] were reported to form hydrogels based on inclusion complexation between α-CD and PEO. Similar complexation was also reported for poly(ethylene oxide)-*b*-poly(ε-caprolactone) (PEO-PCL) diblock copolymers. CDs were shown to recognize and form complexes selectively with different polymer blocks to form supramolecular structures.[139,150,151]

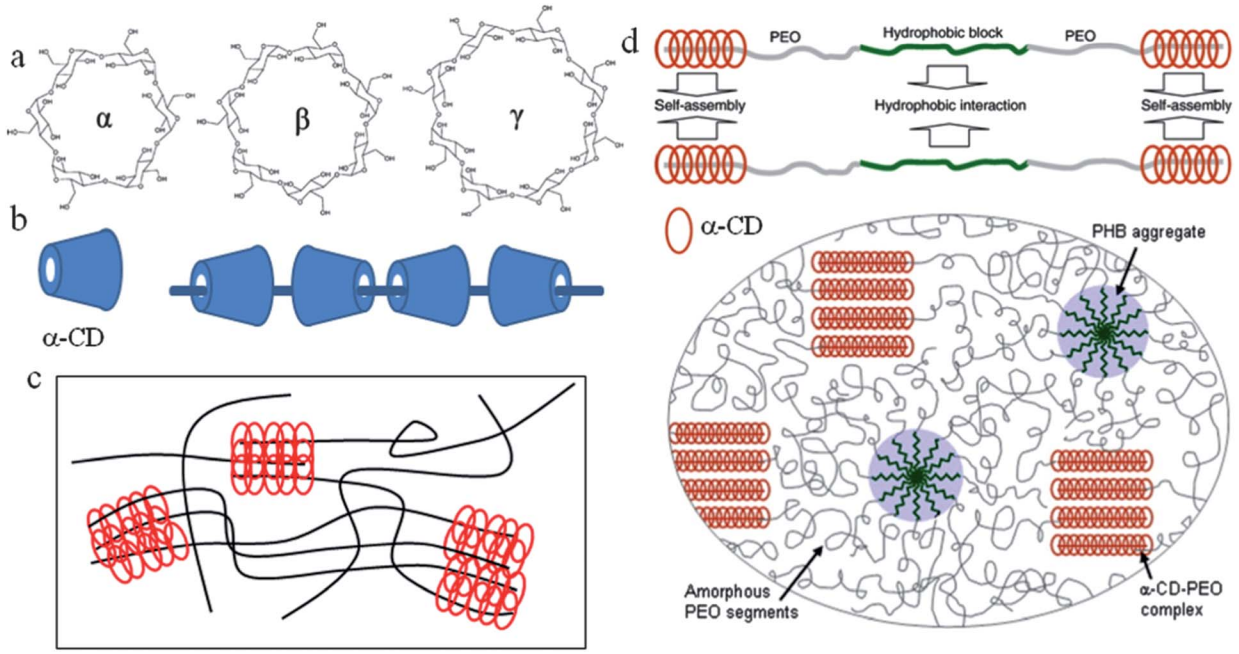

Fig. 8 (a) Chemical structures of α, β, and γ–CD. (b–c) Schematic of α-CD on PEO chain and self-assembled network for α-CD-PEO. (d–e) Schematic illustrations of proposed structure of the α-CD-PEO-PHB-PEO inclusion complex (d) and network formation (c). Reproduced from Li *et al.*, ref. 146, with permission.

Shear-thinning hydrogels based on the self-assembly of the inclusion complexes between CD with biodegradable polymers have promising potential for biomedical applications such as injectable drug and gene delivery systems.[138,139,152,153] However, the majority of work on injectable drug delivery systems is limited to *in vitro* evaluation using model drugs such as fluorescein isothiocyanate labelled dextran (dextran-FITC) and BSA-FITC. For instance, in α-CD/PEO hydrogels, dextran-FITC release rates decreased sharply with increasing PEO molecular weight from 8 up to 35 kDa and was steady for PEO molecular weight between 35 to 100 kDa.[154] Furthermore, the drug release kinetics were found to be determined by the erosion of the hydrogels due to dethreading of PEO chains from the cavities of CDs, not by the molecular weight of the drug.[154] However, the use of these hydrogels for drug delivery is challenging due to fast release kinetics for low molecular weight PEO, and biodegradability issues for high molecular weight PEO.[138] Similar long-term instability problems were reported for hydrogels formed by α-CD and PEO-PPO-PEO determined mainly by the PEO molecular weight and block composition, indicating the importance of balance between the PEO and PPO blocks. Hydrogels with copolymers $EO_{10}PO_{44}EO_{10}$ showed sustained long-term release of BSA-FITC.[155] Supporting the inclusion complexes with hydrophobic aggregation of the unthreaded polymer blocks eliminated these stability issues as explained above. α-CD/PEO-PHB-PEO (5k-3k-5k) hydrogels were more stable with sustained release of FITC-dextran for over 1 month,[146] whereas much higher molecular weight α-CD/PEO (35kDa) dissociated in 5 days.[154] Therefore, α-CD/PEO-PHB-PEO shows a considerable improvement in behavior.

We would like to note that CD-based shear-thinning hydrogels for injectable drug delivery is an emerging field with promising potential but with many questions and challenges. For instance, the reported shear-thinning (~20 min) and recovery kinetics (several hours)[154] are much slower than the other injectable systems (generally within minutes). Enhanced material design routes are needed to develop stable hydrogels with good biocompatibility and biodegradability. Finally, *in vivo* studies are extremely necessary to test the hydrogel stability, release efficiency and most importantly, the toxicity.

4. Conclusions and future directions

In summary, a wide range of shear-thinning systems are being developed that self-assemble to form network structures under physiological conditions, flow under moderate pressure (during injection), and self-heal (after injection). These systems are highly tunable and amenable to the incorporation of biological functionality, such as matrix degradation and adhesion sites. Although the use of these systems as injectable hydrogels in biomedicine is very recent and mostly limited to *in vitro* studies, the majority of these systems are potentially suitable for tissue-engineering and molecule delivery applications.

In many currently used injectable hydrogels, cargo and polymer precursors are injected in liquid form and polymerized *in situ* by free radicals and chemical linkers, or by changes in pH, temperature, or ionic strength.[156,157] However, delivery will fail if polymerization occurs too rapidly and gelation occurs within the delivery device. If polymerization occurs too slowly, there may be significant cargo loss and leaking from the target site. Ideally, pseudoplastic and rapidly self-healing hydrogels will not have these kinetic-related issues since they constantly flow when subjected to shear-stress, and quickly self-heal once shear-stress

ceases. Also, *in vitro* cargo encapsulation methods may assist in improving experimental repeatability.[50]

Although this review shows the potential use and advantages of shear-thinning systems in drug delivery and cellular encapsulation and delivery, only a handful of systems have been reported to be used *in vivo* due to compatibility of physical, structural and mechanical properties. One significant limiting factor with current systems is their relatively poor mechanical properties due to weak physical cross-linking interactions, as compared to covalent bonding. One approach to overcome this is temporal stiffening *via* triggered covalent bond formation after shear recovery. Another important limitation is prolonged shear-thinning and -recovery kinetics (such as in the case of CD-based systems), which may be improved with the identification of more specific interactions that recover more quickly. Moreover, as shear-thinning hydrogels rely on physical association it is critical to obtain gels at physiological pH and temperature, and maintain their structural stability and inertness in the presence of charged molecules and/or ECM components. It is also important to achieve stable hydrogels with tunable gel erosion rates, which is crucial for delivery applications. Finally, *in vivo* studies are needed to test the hydrogel stability, release/delivery efficiency and most importantly, the toxicity. Along with this, imaging approaches will prove useful to track materials during injection and with erosion. Therefore, further improvements in material design to obtain enhanced mechanical properties, stability and biocompatibility as well as tunable gelation and self-healing kinetics and biodegradability are required for widespread utility of shear-thinning hydrogels for biomedical applications.

Acknowledgements

We are grateful for support from a Fellowship in Science and Engineering from the David and Lucile Packard Foundation (JAB) and a CAREER award (JAB) and Graduate Research Fellowship (HDL) from the National Science Foundation.

References

1 J. A. Burdick and G. D. Prestwich, *Adv. Mater.*, 2011, **23**, H41–H56.
2 S. Khetan and J. A. Burdick, *Soft Matter*, 2011, **7**, 830–838.
3 M. Guvendiren and J. A. Burdick, *Biomaterials*, 2010, **31**, 6511–6518.
4 R. A. Marklein and J. A. Burdick, *Adv. Mater.*, 2010, **22**, 175–189.
5 S. M. Dellatore, A. S. Garcia and W. M. Miller, *Curr. Opin. Biotechnol.*, 2008, **19**, 534–540.
6 J. A. Hubbell, *Bio-Technol.*, 1995, **13**, 565–576.
7 J. D. Kretlow, L. Klouda and A. G. Mikos, *Adv. Drug Delivery Rev.*, 2007, **59**, 263–273.
8 C. Chung and J. A. Burdick, *Tissue Eng. A*, 2009, **15**, 243–254.
9 Y. Yeo, W. Geng, T. Ito, D. S. Kohane, J. A. Burdick and M. Radisic, *J. Biomed. Mater. Res., Part B*, 2007, **81B**, 312–322.
10 A. Khademhosseini, G. Eng, J. Yeh, J. Fukuda, J. Blumling, III, R. Langer and J. A. Burdick, *J. Biomed. Mater. Res., Part A*, 2006, **79A**, 522–532.
11 J. A. Burdick and K. S. Anseth, *Biomaterials*, 2002, **23**, 4315–4323.
12 N. A. Peppas, *Curr. Opin. Colloid Interface Sci.*, 1997, **2**, 531–537.
13 P. Gupta, K. Vermani and S. Garg, *Drug Discovery Today*, 2002, **7**, 569–579.
14 A. K. Bajpai, S. K. Shukla, S. Bhanu and S. Kankane, *Prog. Polym. Sci.*, 2008, **33**, 1088–1118.
15 L. E. Bromberg and E. S. Ron, *Adv. Drug Delivery Rev.*, 1998, **31**, 197–221.
16 N. Artzi, T. Shazly, A. B. Baker, A. Bon and E. R. Edelman, *Adv. Mater.*, 2009, **21**, 3399.
17 N. A. Peppas and J. J. Sahlin, *Biomaterials*, 1996, **17**, 1553–1561.
18 M. Guvendiren, D. A. Brass, P. B. Messersmith and K. R. Shull, *J. Adhes.*, 2009, **85**, 631–645.
19 M. Guvendiren, P. B. Messersmith and K. R. Shull, *Biomacromolecules*, 2008, **9**, 122–128.
20 B. Zhao and J. S. Moore, *Langmuir*, 2001, **17**, 4758–4763.
21 D. J. Beebe, J. S. Moore, J. M. Bauer, Q. Yu, R. H. Liu, C. Devadoss and B. H. Jo, *Nature*, 2000, **404**, 588.
22 A. Sidorenko, T. Krupenkin, A. Taylor, P. Fratzl and J. Aizenberg, *Science*, 2007, **315**, 487–490.
23 J. L. Ifkovits and J. A. Burdick, *Tissue Eng.*, 2007, **13**, 2369–2385.
24 L. Klouda and A. G. Mikos, *Eur. J. Pharm. Biopharm.*, 2008, **68**, 34–45.
25 B. Jeong, S. W. Kim and Y. H. Bae, *Adv. Drug Delivery Rev.*, 2002, **54**, 37–51.
26 E. Ruel-Gariepy and J. C. Leroux, *Eur. J. Pharm. Biopharm.*, 2004, **58**, 409–426.
27 S. Dai, P. Ravi, K. C. Tam, B. W. Mao and L. H. Gang, *Langmuir*, 2003, **19**, 5175–5177.
28 P. Ravi, C. Wang, K. C. Tam and L. H. Gan, *Macromolecules*, 2003, **36**, 173–179.
29 E. Westhaus and P. B. Messersmith, *Biomaterials*, 2001, **22**, 453–462.
30 A. Rozier, C. Mazuel, J. Grove and B. Plazonnet, *Int. J. Pharm.*, 1989, **57**, 163–168.
31 G. Tae, J. A. Kornfield and J. A. Hubbell, *Biomaterials*, 2005, **26**, 5259–5266.
32 M. Guvendiren and K. R. Shull, *Soft Matter*, 2007, **3**, 619–626.
33 S. M. Loverde, V. Ortiz, R. D. Kamien, M. L. Klein and D. E. Discher, *Soft Matter*, 2010, **6**, 1419–1425.
34 L. Yu and J. Ding, *Chem. Soc. Rev.*, 2008, **37**, 1473–1481.
35 J. S. Temenoff and A. G. Mikos, *Biomaterials*, 2000, **21**, 2405–2412.
36 C. Q. Yan, A. Altunbas, T. Yucel, R. P. Nagarkar, J. P. Schneider and D. J. Pochan, *Soft Matter*, 2010, **6**, 5143–5156.
37 L. Haines-Butterick, K. Rajagopal, M. Branco, D. Salick, R. Rughani, M. Pilarz, M. S. Lamm, D. J. Pochan and J. P. Schneider, *Proc. Natl. Acad. Sci. U. S. A.*, 2007, **104**, 7791–7796.
38 Y. L. Chiu, S. C. Chen, C. J. Su, C. W. Hsiao, Y. M. Chen, H. L. Chen and H. W. Sung, *Biomaterials*, 2009, **30**, 4877–4888.
39 G. A. Silva, C. Czeisler, K. L. Niece, E. Beniash, D. A. Harrington, J. A. Kessler and S. I. Stupp, *Science*, 2004, **303**, 1352–1355.
40 B. D. Olsen, J. A. Kornfield and D. A. Tirrell, *Macromolecules*, 2010, **43**, 9094–9099.
41 L. Aulisa, H. Dong and J. D. Hartgerink, *Biomacromolecules*, 2009, **10**, 2694–2698.
42 S. S. Santoso, S. Vauthey and S. Zhang, *Curr. Opin. Colloid Interface Sci.*, 2002, **7**, 262–266.
43 D. W. P. M. Löwik and J. C. M. Van Hest, *Chem. Soc. Rev.*, 2004, **33**, 234–245.
44 X. Zhao, F. Pan, H. Xu, M. Yaseen, H. Shan, C. A. E. Hauser, S. Zhang and J. R. Lu, *Chem. Soc. Rev.*, 2010, **39**, 3480–3498.
45 X. Zhao and S. Zhang, *Trends Biotechnol.*, 2004, **22**, 470–476.
46 F. Versluis, H. R. Marsden and A. Kros, *Chem. Soc. Rev.*, 2010, **39**, 3434–3444.
47 I. W. Hamley, *Soft Matter*, 2011, **7**, 4122–4138.
48 S. Cavalli and A. Kros, *Adv. Mater.*, 2008, **20**, 627–631.
49 S. Banta, I. R. Wheeldon and M. Blenner, *Annu. Rev. Biomed. Eng.*, 2010, **12**, 167–186.
50 C. Q. Yan and D. J. Pochan, *Chem. Soc. Rev.*, 2010, **39**, 3528–3540.
51 R. J. Mart, R. D. Osborne, M. M. Stevens and R. V. Ulijn, *Soft Matter*, 2006, **2**, 822–835.
52 K. Rajagopal and J. P. Schneider, *Curr. Opin. Struct. Biol.*, 2004, **14**, 480–486.
53 L. A. Haines, K. Rajagopal, B. Ozbas, D. A. Salick, D. J. Pochan and J. P. Schneider, *J. Am. Chem. Soc.*, 2005, **127**, 17025–17029.
54 D. J. Pochan, J. P. Schneider, J. Kretsinger, B. Ozbas, K. Rajagopal and L. Haines, *J. Am. Chem. Soc.*, 2003, **125**, 11802–11803.
55 K. Rajagopal, B. Ozbas, D. J. Pochan and J. P. Schneider, *Eur. Biophys. J.*, 2006, **35**, 162–169.
56 R. V. Rughani, D. A. Salick, M. S. Lamm, T. Yucel, D. J. Pochan and J. P. Schneider, *Biomacromolecules*, 2009, **10**, 1295–1304.
57 J. P. Schneider, D. J. Pochan, B. Ozbas, K. Rajagopal, L. Pakstis and J. Kretsinger, *J. Am. Chem. Soc.*, 2002, **124**, 15030–15037.
58 B. Ozbas, K. Rajagopal, J. P. Schneider and D. J. Pochan, *Physical Review Letters*, 2004, **93**, 268106.

59 K. Rajagopal, M. S. Lamm, L. A. Haines-Butterick, D. J. Pochan and J. P. Schneider, *Biomacromolecules*, 2009, **10**, 2619–2625.
60 B. Ozbas, J. Kretsinger, K. Rajagopal, J. P. Schneider and D. J. Pochan, *Macromolecules*, 2004, **37**, 7331–7337.
61 R. V. Rughani and J. R. Schneider, *MRS Bull.*, 2008, **33**, 530–535.
62 J. K. Kretsinger, L. A. Haines, B. Ozbas, D. J. Pochan and J. P. Schneider, *Biomaterials*, 2005, **26**, 5177–5186.
63 M. C. Branco and J. P. Schneider, *Acta Biomater.*, 2009, **5**, 817–831.
64 L. A. Haines-Butterick, D. A. Salick, D. J. Pochan and J. P. Schneider, *Biomaterials*, 2008, **29**, 4164–4169.
65 D. A. Salick, J. K. Kretsinger, D. J. Pochan and J. P. Schneider, *J. Am. Chem. Soc.*, 2007, **129**, 14793–14799.
66 A. Altunbas, S. J. Lee, S. A. Rajasekaran, J. P. Schneider and D. J. Pochan, *Biomaterials*, 2011, **32**, 5906–5914.
67 B. B. Aggarwal, A. Kumar and A. C. Bharti, *Anticancer Research*, 2003, **23**, 363–398.
68 Y. J. Surh, *Food Chem. Toxicol.*, 2002, **40**, 1091–1097.
69 A. J. Ruby, G. Kuttan, K. Dinesh Babu, K. N. Rajasekharan and R. Kuttan, *Cancer Lett.*, 1995, **94**, 79–83.
70 R. C. Lantz, G. J. Chen, A. M. Solyom, S. D. Jolad and B. N. Timmermann, *Phytomedicine*, 2005, **12**, 445–452.
71 R. V. Rughani, M. C. Branco, D. J. Pochan and J. P. Schneider, *Macromolecules*, 2010, **43**, 7924–7930.
72 D. A. Salick, D. J. Pochan and J. P. Schneider, *Adv. Mater.*, 2009, **21**, 4120.
73 R. V. Rughani, D. A. Salick, M. S. Lamm, T. Yucel, D. J. Pochan and J. P. Schneider, *Biomacromolecules*, 2009, **10**, 1295–1304.
74 H. Dong, S. E. Paramonov, L. Aulisa, E. L. Bakota and J. D. Hartgerink, *J. Am. Chem. Soc.*, 2007, **129**, 12468–12472.
75 M. S. Lamm, K. Rajagopal, J. P. Schneider and D. J. Pochan, *J. Am. Chem. Soc.*, 2005, **127**, 16692–16700.
76 Y. Wang, E. Bakota, B. H. J. Chang, M. Entman, J. D. Hartgerink and F. R. Danesh, *J. Am. Soc. Nephrol.*, 2011, **22**, 704–717.
77 K. Pagel, S. C. Wagner, K. Samedov, H. Von Berlepsch, C. Böttcher and B. Koksch, *J. Am. Chem. Soc.*, 2006, **128**, 2196–2197.
78 S. E. Paramonov, H. W. Jun and J. D. Hartgerink, *J. Am. Chem. Soc.*, 2006, **128**, 7291–7298.
79 K. M. Galler, L. Aulisa, K. R. Regan, R. N. D'Souza and J. D. Hartgerink, *J. Am. Chem. Soc.*, 2010, **132**, 3217–3223.
80 M. Miura, S. Gronthos, M. Zhao, B. Lu, L. W. Fisher, P. G. Robey and S. Shi, *Proc. Natl. Acad. Sci. U. S. A.*, 2003, **100**, 5807–5812.
81 E. L. Bakota, Y. Wang, F. R. Danesh and J. D. Hartgerink, *Biomacromolecules*, 2011, **12**, 1651–1657.
82 B. Bi, R. Schmitt, M. Israilova, H. Nishio and L. G. Cantley, *J. Am. Soc. Nephrol.*, 2007, **18**, 2486–2496.
83 B. D. Humphreys and J. V. Bonventre, *Annu. Rev. Med.*, 2008, **59**, 311–325.
84 B. Imberti, M. Morigi, S. Tomasoni, C. Rota, D. Corna, L. Longaretti, D. Rottoli, F. Valsecchi, A. Benigni, J. Wang, M. Abbate, C. Zoja and G. Remuzzi, *J. Am. Soc. Nephrol.*, 2007, **18**, 2921–2928.
85 Y. M. Zhang, J. Bo, G. E. Taffet, J. Chang, J. Shi, A. K. Reddy, L. H. Michael, M. D. Schneider, M. L. Entman, R. J. Schwartz and L. Wei, *FASEB J.*, 2006, **20**, 916–925.
86 B. E. Reubinoff, M. F. Pera, C. Y. Fong, A. Trounson and A. Bongso, *Nat. Biotechnol.*, 2000, **18**, 399–404.
87 M. J. Webber, X. Han, S. N. Prasanna Murthy, K. Rajangam, S. I. Stupp and J. W. Lomasney, *J. Tissue Eng. Regener. Med.*, 2010, **4**, 600–610.
88 S. Ramachandran, J. Trewhella, Y. Tseng and Y. B. Yu, *Chem. Mater.*, 2006, **18**, 6157–6162.
89 S. Ramachandran, P. Flynn, Y. Tseng and Y. B. Yu, *Chem. Mater.*, 2005, **17**, 6583–6588.
90 M. R. Caplan, E. M. Schwartzfarb, S. Zhang, R. D. Kamm and D. A. Lauffenburger, *J. Biomater. Sci., Polym. Ed.*, 2002, **13**, 225–236.
91 F. Guzmán, S. Barberis and A. Illanes, *Electron. J. Biotechnol.*, 2007, **10**, 279–314.
92 J. A. Brannigan and A. J. Wilkinson, *Nat. Rev. Mol. Cell Biol.*, 2002, **3**, 964–970.
93 C. Foo, J. S. Lee, W. Mulyasasmita, A. Parisi-Amon and S. C. Heilshorn, *Proc. Natl. Acad. Sci. U. S. A.*, 2009, **106**, 22067–22072.
94 M. Sudol, H. I. Chen, C. Bougeret, A. Einbond and P. Bork, *FEBS Lett.*, 1995, **369**, 67–71.
95 M. Sudol, P. Bork, A. Einbond, K. Kastury, T. Druck, M. Negrini, K. Huebner and D. Lehman, *J. Biol. Chem.*, 1995, **270**, 14733–14741.
96 M. J. Macias, V. Gervais, C. Civera and H. Oschkinat, *Nat. Struct. Biol.*, 2000, **7**, 375–379.
97 V. Kanelis, D. Rotin and J. D. Forman-Kay, *Nat. Struct. Biol.*, 2001, **8**, 407–412.
98 J. R. Pires, F. Taha-Nejad, F. Toepert, T. Ast, U. Hoffmüller, J. Schneider-Mergener, R. Kühne, M. J. Macias and H. Oschkinat, *J. Mol. Biol.*, 2001, **314**, 1147–1156.
99 K. Saha, A. J. Keung, E. F. Irwin, Y. Li, L. Little, D. V. Schaffer and K. E. Healy, *Biophys. J.*, 2008, **95**, 4426–4438.
100 W. Landschulz, P. Johnson and S. McKnight, *Science*, 1988, **240**, 1759–1764.
101 W. A. Petka, J. L. Harden, K. P. McGrath, D. Wirtz and D. A. Tirrell, *Science*, 1998, **281**, 389–392.
102 S. B. Kennedy, E. R. deAzevedo, W. A. Petka, T. P. Russell, D. A. Tirrell and M. Hong, *Macromolecules*, 2001, **34**, 8675–8685.
103 S. B. Kennedy, K. Littrell, P. Thiyagarajan, D. A. Tirrell and T. P. Russell, *Macromolecules*, 2005, **38**, 7470–7475.
104 L. X. Mi, S. Fischer, B. Chung, S. Sundelacruz and J. L. Harden, *Biomacromolecules*, 2006, **7**, 38–47.
105 S. E. Fischer, X. Liu, H.-Q. Mao and J. L. Harden, *Biomaterials*, 2007, **28**, 3325–3337.
106 W. Shen, J. A. Kornfield and D. A. Tirrell, *Soft Matter*, 2007, **3**, 99–107.
107 W. Shen, R. G. H. Lammertink, J. K. Sakata, J. A. Kornfield and D. A. Tirrell, *Macromolecules*, 2005, **38**, 3909–3916.
108 W. Shen, K. Zhang, J. A. Kornfield and D. A. Tirrell, *Nat. Mater.*, 2006, **5**, 153–158.
109 I. R. Wheeldon, S. Calabrese Barton and S. Banta, *Biomacromolecules*, 2007, **8**, 2990–2994.
110 H. D. Lu, I. R. Wheeldon and S. Banta, *Protein Eng., Des. Sel.*, 2010, **23**, 559–566.
111 I. R. Wheeldon, E. Campbell and S. Banta, *J. Mol. Biol.*, 2009, **392**, 129–142.
112 S. Topp, V. Prasad, G. C. Cianci, E. R. Weeks and J. P. Gallivan, *J. Am. Chem. Soc.*, 2006, **128**, 13994–13995.
113 B. Liu, A. K. Lewis and W. Shen, *Biomacromolecules*, 2009, **10**, 3182–3187.
114 D. Gupta, C. H. Tator and M. S. Shoichet, *Biomaterials*, 2006, **27**, 2370–2379.
115 L. Li, P. M. Thangamathesvaran, C. Y. Yue, K. C. Tam, X. Hu and Y. C. Lam, *Langmuir*, 2001, **17**, 8062–8068.
116 M. C. Jimenez Hamann, E. C. Tsai, C. H. Tator and M. S. Shoichet, *Exp. Neurol.*, 2003, **182**, 300–309.
117 A. S. Rivlin and C. H. Tator, *Surgical Neurology*, 1978, **10**, 39–43.
118 Y. F. Wang, Y. Lapitsky, C. E. Kang and M. S. Shoichet, *J. Controlled Release*, 2009, **140**, 218–223.
119 E. Loizou, P. Butler, L. Porcar and G. Schmidt, *Macromolecules*, 2006, **39**, 1614–1619.
120 A. Nelson and T. Cosgrove, *Langmuir*, 2004, **20**, 10382–10388.
121 A. Nelson and T. Cosgrove, *Langmuir*, 2004, **20**, 2298–2304.
122 P. Schexnailder and G. Schmidt, *Colloid Polym. Sci.*, 2009, **287**, 1–11.
123 V. F. Sechriest, Y. J. Miao, C. Niyibizi, A. Westerhausen-Larson, H. W. Matthew, C. H. Evans, F. H. Fu and J. K. Suh, *J. Biomed. Mater. Res.*, 2000, **49**, 534–541.
124 J. Xi Lu, F. Prudhommeaux, A. Meunier, L. Sedel and G. Guillemin, *Biomaterials*, 1999, **20**, 1937–1944.
125 R. A. A. Muzzarelli, *Carbohydr. Polym.*, 1993, **20**, 7–16.
126 P. J. Schexnailder, A. K. Gaharwar, R. L. Bartlett Ii, B. L. Seal and G. Schmidt, *Macromol. Biosci.*, 2010, **10**, 1416–1423.
127 Q. Jin, P. Schexnailder, A. K. Gaharwar and G. Schmidt, *Macromol. Biosci.*, 2009, **9**, 1028–1035.
128 A. K. Gaharwar, P. J. Schexnailder, B. P. Kline and G. Schmidt, *Acta Biomater.*, 2011, **7**, 568–577.
129 A. K. Gaharwar, P. J. Schexnailder, Q. Jin, C.-J. Wu and G. Schmidt, *ACS Appl. Mater. Interfaces*, 2010, **2**, 3119–3127.
130 Q. Wang, L. Wang, M. S. Detamore and C. Berkland, *Adv. Mater.*, 2008, **20**, 236–239.
131 Q. Wang, J. Wang, Q. Lu, M. S. Detamore and C. Berkland, *Biomaterials*, 2010, **31**, 4980–4986.
132 Q. Wang, S. Jamal, M. S. Detamore and C. Berkland, *J. Biomed. Mater. Res., Part A*, 2011, **96A**, 520–527.

133 M. E. Keegan, J. L. Falcone, T. C. Leung and W. M. Saltzman, *Macromolecules*, 2004, **37**, 9779–9784.
134 L. Shi and C. Berkland, *Adv. Mater.*, 2006, **18**, 2315–2319.
135 L. Shi and C. Berkland, *Macromolecules*, 2007, **40**, 4635–4643.
136 K. L. C. J. Coester, H. Von Briesen and J. Kreuter, *J. Microencapsulation*, 2000, **17**, 187–193.
137 T. G. Shutava, S. S. Balkundi, P. Vangala, J. J. Steffan, R. L. Bigelow, J. A. Cardelli, D. P. O'Neal and Y. M. Lvov, *ACS Nano*, 2009, **3**, 1877–1885.
138 J. Li and X. J. Loh, *Adv. Drug Delivery Rev.*, 2008, **60**, 1000–1017.
139 J. Araki and K. Ito, *Soft Matter*, 2007, **3**, 1456–1473.
140 A. Harada, J. Li and M. Kamachi, *Nature*, 1992, **356**, 325–327.
141 A. Harada, J. Li and M. Kamachi, *Nature*, 1994, **370**, 126–128.
142 A. Harada, J. Li and M. Kamachi, *Macromolecules*, 1993, **26**, 5698–5703.
143 L. H. He, J. Huang, Y. M. Chen and L. P. Liu, *Macromolecules*, 2005, **38**, 3351–3355.
144 A. Harada, M. Okada, J. Li and M. Kamachi, *Macromolecules*, 1995, **28**, 8406–8411.
145 J. Li, X. P. Ni, Z. H. Zhou and K. W. Leong, *J. Am. Chem. Soc.*, 2003, **125**, 1788–1795.
146 J. Li, X. Li, X. P. Ni, X. Wang, H. Z. Li and K. W. Leong, *Biomaterials*, 2006, **27**, 4132–4140.
147 K. M. Huh, T. Ooya, W. K. Lee, S. Sasaki, I. C. Kwon, S. Y. Jeong and N. Yui, *Macromolecules*, 2001, **34**, 8657–8662.
148 K. M. Huh, Y. W. Cho, H. Chung, I. C. Kwon, S. Y. Jeong, T. Ooya, W. K. Lee, S. Sasaki and N. Yui, *Macromol. Biosci.*, 2004, **4**, 92–99.
149 T. Nakama, T. Ooya and N. Yui, *Polym. J.*, 2004, **36**, 338–344.
150 A. Harada and K. Kataoka, *Prog. Polym. Sci.*, 2006, **31**, 949–982.
151 A. Harada, *Coord. Chem. Rev.*, 1996, **148**, 115–133.
152 A. Harada, Y. Takashima and H. Yamaguchi, *Chem. Soc. Rev.*, 2009, **38**, 875–882.
153 F. Hirayama and K. Uekama, *Adv. Drug Delivery Rev.*, 1999, **36**, 125–141.
154 J. Li, X. P. Ni and K. W. Leong, *J. Biomed. Mater. Res.*, 2003, **65A**, 196–202.
155 X. P. Ni, A. Cheng and J. Li, *J. Biomed. Mater. Res., Part A*, 2009, **88A**, 1031–1036.
156 M. K. Nguyen and D. S. Lee, *Macromol. Biosci.*, 2010, **10**, 563–579.
157 H. Tan and K. G. Marra, *Materials*, 2010, **3**, 1746–1767.

